



Plant Phenology of High-Elevation Meadows: Assessing Spectral Responses of Grazed Meadows★

Authors: Snyder, Keirith A., Richardson, William, Browning, Dawn M., Lieurance, Wade, and Stringham, Tamzen K.

Source: Rangeland Ecology and Management, 87(1) : 69-82

Published By: Society for Range Management

URL: <https://doi.org/10.1016/j.rama.2022.12.001>

BioOne Complete (complete.BioOne.org) is a full-text database of 200 subscribed and open-access titles in the biological, ecological, and environmental sciences published by nonprofit societies, associations, museums, institutions, and presses.

Your use of this PDF, the BioOne Complete website, and all posted and associated content indicates your acceptance of BioOne's Terms of Use, available at www.bioone.org/terms-of-use.

Usage of BioOne Complete content is strictly limited to personal, educational, and non - commercial use. Commercial inquiries or rights and permissions requests should be directed to the individual publisher as copyright holder.

BioOne sees sustainable scholarly publishing as an inherently collaborative enterprise connecting authors, nonprofit publishers, academic institutions, research libraries, and research funders in the common goal of maximizing access to critical research.



Contents lists available at ScienceDirect

Rangeland Ecology & Management

journal homepage: www.elsevier.com/locate/rama

Original Research

Plant Phenology of High-Elevation Meadows: Assessing Spectral Responses of Grazed Meadows [☆]

Keirith A. Snyder^{a,*}, William Richardson^b, Dawn M. Browning^c, Wade Lieurance^b, Tamzen K. Stringham^b

^a USDA Agricultural Research Service, Great Basin Rangelands Research Unit, Reno, NV, 89512, USA

^b University Nevada Reno, Department of Agriculture, Veterinary and Rangeland Science, Reno, NV, 89557, USA

^c USDA Agricultural Research Service, Jornada Experimental Range, Las Cruces, NM, 88003, USA



ARTICLE INFO

Article history:

Received 30 September 2021

Revised 1 December 2022

Accepted 5 December 2022

Key Words:

grazing management
gross primary production (GPP)
groundwater-dependent ecosystems
Landsat NDVI
PhenoCam GCC

ABSTRACT

Groundwater-dependent ecosystems are biologically diverse and productive ecosystems but constitute a small fraction of total land area in semiarid regions. Efforts to link remotely sensed data from satellite-based platforms to measurements of vegetation structure and function at smaller spatial scales have increasingly received attention, due to the need to manage diverse landscapes at scales relevant to management. In the semiarid western United States, grazing is a dominant land use and meadows can receive a high degree of grazing pressure. In this study we examined satellite-based and near-surface imagery to determine if they were useful in assessing grazed systems with different grazing management. We compared meadows that were chronically grazed by feral horses in conjunction with periodic cattle grazing to a meadow managed and grazed by cattle only. We examined the agreement between near-surface digital cameras (PhenoCams) and satellite-based indices of greenness and production for meadows in the Central Great Basin, United States. We also verified them with field-collected data on percent foliar cover by dominant functional groups. There was strong agreement between the Landsat normalized difference vegetation index and PhenoCam Green Chromatic Coordinate (GCC) (Pearson's $r \geq 0.61$). Gross primary production modeled using Landsat satellite imagery and integrated over the growing season had a strong linear relationship with GCC integrated over the growing season ($R^2 = 0.89$). Furthermore, despite differences in spatial and temporal resolution, integrated metrics from both platforms were able to discern differences in grazing pressure. Meadows with chronic feral horse grazing plus 3 mo of livestock grazing had reduced integrated gross primary production and GCC in comparison with a meadow that had short-term grazing (for 2 mo) by livestock only. The ability to detect differences in grazed systems from PhenoCams and satellite platforms provides important tools for quantifying the effects of grazing in groundwater-dependent ecosystems.

Published by Elsevier Inc. on behalf of The Society for Range Management.

This is an open access article under the CC BY-NC-ND license

(<http://creativecommons.org/licenses/by-nc-nd/4.0/>)

Introduction

Phenology is the study of relationships between periodic biological phenomena and the climatic factors that influence them. Since the beginning of the 21st century, monitoring phenology

from near-surface cameras and satellite-based remote sensing has received increased attention, due in part to realized and projected changes in global climate, which necessitate understanding changes in plant phenology (Cleland et al. 2007; Bradley and Mustard 2008; Brown et al. 2016; Tang et al. 2016). Changes in timing of vegetation green up, peak production, and length of the growing season have important implications for carbon storage, multitrophic interactions between vegetation and wildlife, and available forage for livestock (Caldwell 1984; Briske and Richards 1995; Bailey 2004). Near-surface digital cameras capture dynamics at finer spatial scales and greater temporal resolution than those discerned via satellite platforms (Browning et al. 2017, 2019). Enhanced temporal and spatial resolutions come at the cost of

[☆] Funding for the project was provided by the Bureau of Land Management's "Soil, Water and Riparian Monitoring and Research in Nevada" project L19PG00078 and Great Basin CESU "Nevada Forest and Rangeland Research Project" project L15AC00075. DMB was supported by CRIS project 3050-11210-009-00D.

* Correspondence: Keirith A. Snyder, USDA Agricultural Research Service, Great Basin Rangelands Research Unit, Reno, NV 89512, USA.

E-mail address: keirith.snyder@usda.gov (K.A. Snyder).

<https://doi.org/10.1016/j.rama.2022.12.001>

1550-7424/Published by Elsevier Inc. on behalf of The Society for Range Management. This is an open access article under the CC BY-NC-ND license

(<http://creativecommons.org/licenses/by-nc-nd/4.0/>)

diminished feasibility of capturing dynamics across broad spatial scales or geographic extents. Satellite-based remote sensing platforms provide critical information at extents ranging from landscape, to regional, and on to global. The challenge is to blend these multiple scales of measurement and verify them with the most relevant data collected (typically) in the field and to identify whether and how remotely sensed metrics correlate with field data and derive relationships that facilitate extrapolation (Browning et al. 2015).

Although arid and semiarid groundwater-dependent systems are a small fraction ($\approx 1\%$) of the total land area, they provide a disproportionate amount of ecosystem goods and services (Sada 2008). Their importance is recognized worldwide, as is their susceptibility to human-caused degradation (Rohde et al. 2017). Groundwater-dependent ecosystems (GDEs) include riparian areas, meadows, and springs that rely on near-surface shallow groundwater to support vegetation. GDEs support greater levels of vegetation density due to the near-surface water than the more xeric upland ecosystems (Naumburg et al. 2005). They provide a disproportionate amount of forage for a taxonomically diverse species, are critical habitat for wildlife, and have high biological diversity (Kauffman and Krueger 1984; Naiman et al. 1993; Sada 2008; Fesenmyer et al. 2018). GDEs are receiving increased attention, in response to growing threats such as increasing air temperatures and demands for water and livestock products and the importance of these systems for maintaining floral and faunal diversity (Lowry et al. 2011).

Many mountain ranges in the semiarid western United States are characterized by wet winters and dry summers, with ecosystems that rely on snowmelt and groundwater during the summer dry season; mountain meadows are an important subset of GDEs (Lowry et al. 2011). Annual fluctuations in precipitation and temperature will cause meadows to naturally expand during wet periods and contract during dry periods (Naumburg et al. 2005; Huntington et al. 2016). In addition to natural variation, demands on limited water resources in these areas, such as groundwater pumping for agriculture, water for human consumption, and livestock water, can place these systems at risk (Devitt et al. 2011; Devitt et al. 2018). The Great Basin is characterized by north-to-south trending mountain ranges interspersed with aggraded valleys. It is a cold high-elevation desert, where snowfall varies with elevation; historically across the region, approximately 75% of the precipitation has fallen as snow (Klos et al. 2014). Precipitation that falls as rainfall is generally minimal for deep groundwater recharge below the rooting zone (Scanlon et al. 2005; Scanlon et al. 2009). Great Basin GDEs are tightly coupled to precipitation to recharge groundwater, primarily from mountain recharge associated with snowmelt (Harrill et al. 1983). Degradation of meadows caused by channel incision and subsequent declines in depth to groundwater can push these systems to cross hydrologic thresholds that are difficult to restore (Kauffman and Krueger 1984; Stringham et al. 2001; Fesenmyer et al. 2018).

GDEs in the Great Basin are of conservation concern, and monitoring these systems is an ongoing research focus (Brown et al. 2011; Badik et al. 2019). These ecosystems can be extremely sensitive to disturbance and interannual precipitation variability, which may lead to declines in ecosystem services (e.g., soil loss, limited forage capacity, water storage) (Reynolds et al. 2007; Zhao et al. 2017). Grazing and other disturbances have the potential to affect the high temporal variability that accompanies resource availability in these areas (Lebon et al. 2014). Assessing their current ecological condition is a prerequisite to address effective management strategies of GDEs. The ecological condition of GDEs can be assessed by field monitoring (Elmore et al. 2006; Pérez Hoyos et al. 2016). Field methods can be quite time-consuming and spatially limited. Efforts to employ remotely sensed data from satellite-

based sensors to link land surface dynamics, vegetation structure, and ecosystem function have become increasingly sophisticated (Hufkens et al. 2016) and, at the same time, publicly available (ClimateEngine.org). Two recent reviews have highlighted how remote sensing techniques have been successfully used in a variety of water-limited systems worldwide to identify critical GDEs for management (Eamus et al. 2015; Pérez Hoyos et al. 2016). Recent research in the Great Basin used near-surface cameras (hereafter referred to as PhenoCams) and remotely sensed Landsat imagery to assess the function of meadow GDEs by calculating various indices of meadow greenness and vigor.

The normalized vegetation difference index (NDVI; Tucker et al. 1979) and Green Chromatic Coordinate (GCC; Sonnentag et al. 2012) greenness indices have been shown to be effective at characterizing meadow function in the Great Basin from both the Landsat archive (Huntington et al. 2016; Snyder et al. 2019b) and PhenoCams (Snyder et al. 2016; Snyder et al. 2019b). Relationships between NDVI derived from satellite and gross primary production in western rangelands are mixed due to sparse vegetation cover in many areas (Phillips et al. 2008; Huang et al. 2021). We previously evaluated the ability to determine the relationships between dominant plant communities of the Great Basin with NDVI from PhenoCam imagery and Landsat-derived NDVI (Snyder et al. 2019b). We found that for meadow communities, relationships of NDVI were generally robust for peak of season and start of season; however, there was less agreement with the start and end of fall senescence. Since grazing relies on the whole growing season and upper meadow systems are critical to extend the grazing season for cattle, we chose to evaluate GCC from PhenoCams to evaluate potential differences in grazing pressure. GCC is the most commonly used vegetation index from PhenoCam imagery as it is a proportional measure of relative channel brightness that appears to be robust in reducing noise in the phenology signal from vegetation (Richardson et al. 2009; Sonnentag et al. 2012; Julitta et al. 2014; Brown et al. 2017; Browning et al. 2017; Cremonese et al. 2017; Toda and Richardson 2018; Vrieling et al. 2018; Cui et al. 2019; Burke and Rundquist 2021). In addition, any camera can be used to determine GCC (as no infrared-enabled filter is required) and GCC is computationally easy to calculate, thus making this a practical method that could be employed by land managers. We chose Landsat imagery for its midscale spatial resolution (30×30 m) that most closely matches the size of many meadows in the Great Basin that constitute a mixture of vegetation types (i.e., mixed pixels) (Badgley et al. 2017) and its 16-d revisit frequency that compares with the timescale at which vegetation can respond to environmental triggers.

In the Great Basin, high-elevation meadows ($> 2\,000$ m) exist in many mountain regions of Nevada and are difficult to access. For the remote and extensive nature of the meadow GDEs, time series imagery from PhenoCams and satellite provide ways to assess the rangeland condition of these meadows, thereby potentially providing better tools for natural resource management. In the Great Basin, 70% of the land is public land and managed by federal agencies primarily for grazing, mining, timber, and recreational use (Torregrosa and Devoe 2008). Many meadows are grazed by cattle and are also grazed by feral horses, deer, and other ungulates. Many of the mountain ranges have an overpopulation of feral horses (*Equus ferus caballus*), which can place extreme grazing pressure on rangeland systems (Beever et al. 2018; Garrott 2018). Year-round feral horse grazing can significantly reduce plant height, is notoriously hard to control, and is understudied due to the limited ability to manage feral horse grazing (Beever and Brussard 2000; Boyd et al. 2017; Beever et al. 2018). These landscape-scale challenges provide research imperatives to establish validated tools for remote monitoring of rangelands.

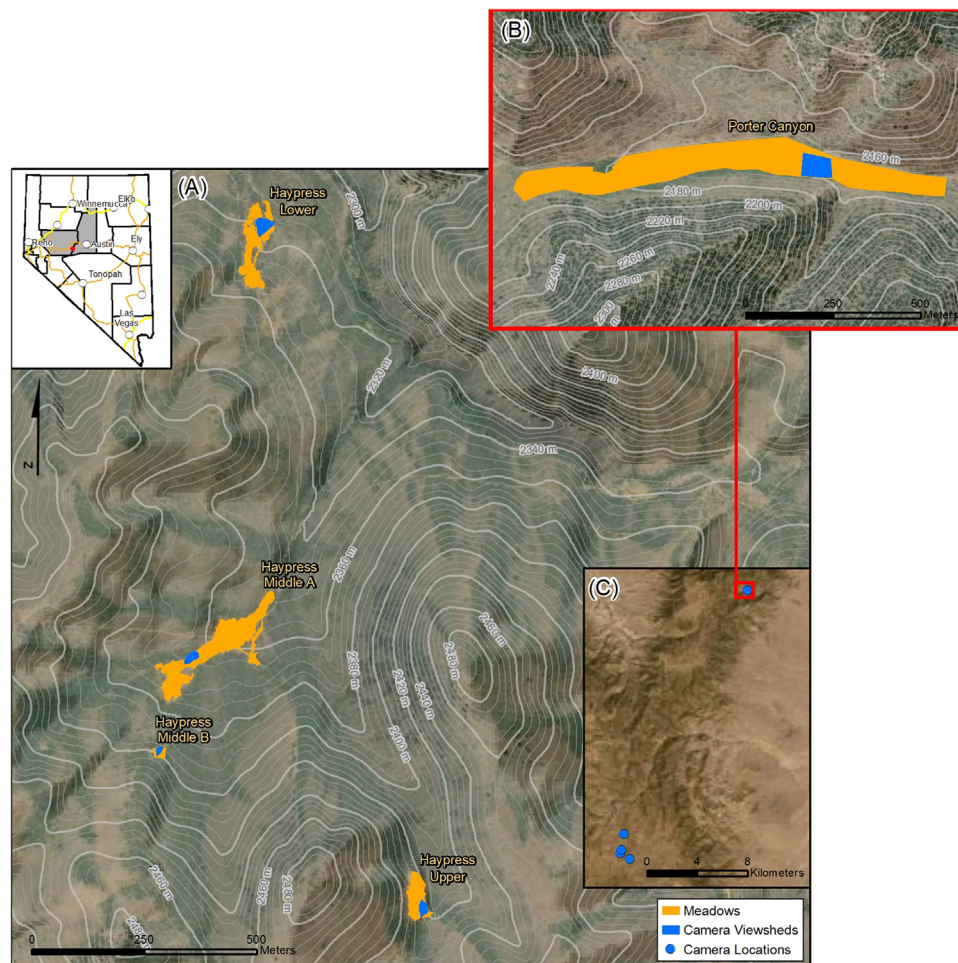


Figure 1. Location of the **A**, Haypress meadow complex and **B**, Porter Canyon Experimental Watershed meadow. Meadows are located in the Desatoya Mountain Range in central Nevada. The extent of the meadows is shown in orange. The camera viewshed (i.e., field of view) of the four PhenoCams is shown in blue. PhenoCam locations are represented by blue dots (C).

A series of high-elevation meadows, referred to as the Haypress meadows, exist in the Desatoya Mountains of the Central Great Basin. These meadows are critical habitat for the at-risk species, the greater sage grouse (*Centrocercus urophasianus*) (Sinai et al. 2017), and are subject to permitted cattle grazing and pressure from a high feral horse population. A 2018 census estimate of feral horse population by the Bureau of Land Management far exceeded the recommended grazing allotment. Federal and state partners have proposed fencing to manage grazing to improve the condition of these meadows. Therefore, assessing baseline land surface condition of these meadows before restoration is prudent to gauge restoration effectiveness. The current study is focused on determining if the degraded ecological condition of these meadows can be quantified by PhenoCams and Landsat metrics of plant greenness and production. In addition, field measurements (such as stubble height and vegetation cover) can be used to enhance these remotely sensed measurements (i.e., PhenoCams and Landsat). Vegetation cover is a commonly used metric in determining recovery rates post grazing disturbance (Bestelmeyer et al. 2013; Khishigbayar et al. 2015), and measuring the stubble height of grazed plants is a useful predictor of when unacceptable impacts (heavy use, trampling, etc.) of grazing are about to occur (General Accounting Office 1988; Hall and Bryant 1995).

Our specific objectives were to determine if we could establish baseline phenology from PhenoCams to quantify seasonal patterns in heavily grazed meadows with three meadow subregions

(i.e., dry, mesic, and wet) before fencing and evaluate the field-estimated canopy cover of functional groups and measured plant height in the four meadows to determine if there were differences between meadows and meadow subregions. We quantified these patterns for four meadows, each of which spanned a wetness gradient and a small-elevation gradient. Furthermore, we quantified relationships between PhenoCam-derived GCC and Landsat-derived NDVI and gross primary production (GPP). Lastly, we examined whether remotely sensed phenology metrics from PhenoCam and Landsat can distinguish differences in grazing pressure.

Methods

Site description

The Desatoya Mountains are in the Central Great Basin, Nevada (39°27'N, 117°36'W; 39°19'N, 117°42'W; Fig. 1). Average annual precipitation for the Haypress meadows during the 30-yr period (1981–2010) obtained from PRISM was 354 mm. Average mean annual temperature was 4.1°C with a minimum temperature of −9.7°C in February and maximum temperature of 24.2°C in July (PRISM Climate Group 2021). The four meadows in the Haypress meadow complex are 1) Upper at 2 395-m elevation, 2) Middle B at 2 365 m, 3) Middle A at 2 340 m, and 4) Lower meadow at 2 295 m. In addition, we used a fifth meadow, Porter Canyon Experimental Watershed meadow at 2 160 m in elevation, in the

Table 1
Meadow and PhenoCam information, including area of the PhenoCam field of view (i.e., camera viewshed), areal extent of the meadows, latitude and longitude of the meadows, elevation of each meadow, and orientation of each PhenoCam.

	Camera viewshed (ha)	Meadow area (ha)	Lat/Long	Elevation	Camera orientation (cardinal direction)
Upper	0.05	0.38	39.317479/-117.697128	2 395	NNE
Middle A	0.06	1.45	39.322538/-117.703238	2 340	NNE
Middle B	0.02	0.07	39.320682/-117.703979	2 365	NNE
Lower	0.11	0.73	39.331126/-117.701456	2 295	NNE
Porter Canyon	0.41	7.48	39.466055/-117.613013	2 160	SSW

latter analyses at the larger meadow scale to determine the effects of different grazing management. The four meadows in Haypress and the meadow in Porter are shown with both the camera field of view (i.e., camera viewshed) and the full extent of the meadow outlined, as determined with field mapping surveys of vegetation (see Fig. 1). The area of the camera viewsheds and full meadows are listed in Table 1. Camera viewsheds ranged from 0.02 to 0.41 ha, and meadows ranged from 0.07 to 7.48 ha (see Table 1).

Grazing in the Haypress meadow complex consisted of year-round grazing by feral horses and cattle grazing. Cattle graze either early or late in the growing season depending on the calendar year. In 2018 approximately 700 cow-calf pairs had access to the Haypress meadows from July to September. The Porter Meadow is completely fenced, and the road is gated, though it is periodically used for managed livestock grazing. There was no feral horse grazing during the period 2015–2018. There were no cattle grazing in 2015 and 2016. The Porter meadow was used in 2017 and 2018 as an area to naturally collect cattle in the August and September. The gate was opened, and cattle entered the meadow and then were removed by the rancher (personal communication, Sam Lossing, ranch manager).

We included the Porter Canyon Experimental Watershed meadow because it was instrumented with a PhenoCam in fall 2014 and has been managed differently for grazing. Therefore, incorporating this meadow for the larger-scale meadow analyses of GCC, GPP, and NDVI provides a grazing contrast and longer time series.

Average annual precipitation for the Porter meadow during the 30-yr period (1981–2010) obtained from PRISM was 341 mm. Average mean annual temperature was 7.9°C with a minimum temperature of –6.8°C in December and maximum temperature of 28.8°C in July. For a full description of Porter Canyon Experimental Watershed, see Snyder et al. (2016, 2019a).

Field survey methods

The line point intercept (LPI) method outlined in the *Monitoring Manual for Grassland, Shrubland, and Savanna Ecosystems* (Herrick et al. 2005) was used to measure percent cover by species via transects that traversed wet, mesic, and dry subregions of each meadow. The LPI method measures canopy by the number of “hits” of a given species out of the total number of points measured along a transect. Number of transects, length of transects, and number of points along transects was dependent on the size and shape of each individual subregion. However, each subregion generated roughly the same number of data points (between 100 and 120). Percent foliar cover was measured in June 2018 and tabulated as the proportion of all hits for a given functional group.

Along each LPI transect, height of plant species was also recorded. At 25%, 50%, and 75% of the total length of each transect, a 1-m hoop was placed and heights of all vegetation within the region were gathered. Heights of plants were recorded bimonthly between June and August of 2018.

PhenoCam imagery

Ground-based cameras (i.e., PhenoCams) were used to determine if multiple photographic images per day could discern differences in plant phenology of heavily grazed meadows. In fall 2017, four PhenoCams were installed in four meadows in the Haypress Meadow complex. We followed the methods for installing and using PhenoCams standardized by the PhenoCam Network (<https://phenocam.nau.edu/webcam> 2018). The Porter Canyon meadow camera was installed in fall of 2014. PhenoCam images were acquired by StarDot NetCam SC 5MP infrared-enabled cameras using a complementary metal oxide semiconductor image sensor at a resolution of 1296 × 960 pixels and a lens focal length of 6.2 mm. Eight RGB images were taken in a two- and one half-hour window with a 30-min interval ranging between 12:00 p.m. and 3:30 p.m. PhenoCam images were manually downloaded monthly in the growing season and every 3 mo in the winter.

We used the R statistical program package, *phenopix* by Filipa et al. (2016), to define areas of interest and extract phenological metrics. Regions of interest were manually defined to be representative of wet, mesic, and dry meadows based on vegetation surveys and maps Fig. 2. We used the average region of interest method where an individual pixel's digital numbers were averaged within the region of interest for each image captured per day. Digital numbers from PhenoCam images range from 0 to 255 and were extracted for red (R), green (G), and blue (B) bands for each color channel. These data are then converted into a relative percent index; we used the GCC:

$$GCC = \frac{GDN}{(RDN + GDN + BDN)} \quad (1)$$

where the digital number of the green channel (GDN) is divided by the sum of all three channels (RDN, GDN, BDN).

To remove images containing snow, we implemented an additional filter not in the *phenopix* package based on the blue chromatic coordinate; see Snyder et al. (2019b) for details. The remaining GCC values for the area-averaged region of interests were filtered using the auto filters available in the *phenopix* package. The filters applied were the night, spline, and max filters, in that order. Filtered subdaily GCC values were processed using a double logistic fit proposed by Gu et al. (2009), and this method was also used to determine seasonal transition dates (i.e., phenophase dates) with 1 000 replications for the uncertainty analysis to discern how well the predicted values fit the observed values. Residuals between fitted and observed were used to generate random noise to the data, and fitting was applied recursively to randomly noised original data. The Gu et al. (2009) threshold method assigns four phenophases: an upturn date when GCC of vegetation begins to increase consistently at the start of the growing season; a stabilization date when vegetation approaches maximum GCC at the peak of the growing season; a downturn date when GCC starts to consistently diminish, indicating the end of the growing season and the beginning of senescence; and a recession date when vegetation is fully senesced and reaches a seasonal low. These upturn and recession dates are fit based on the intercepts of slope of the recovery line (i.e., green up) and the

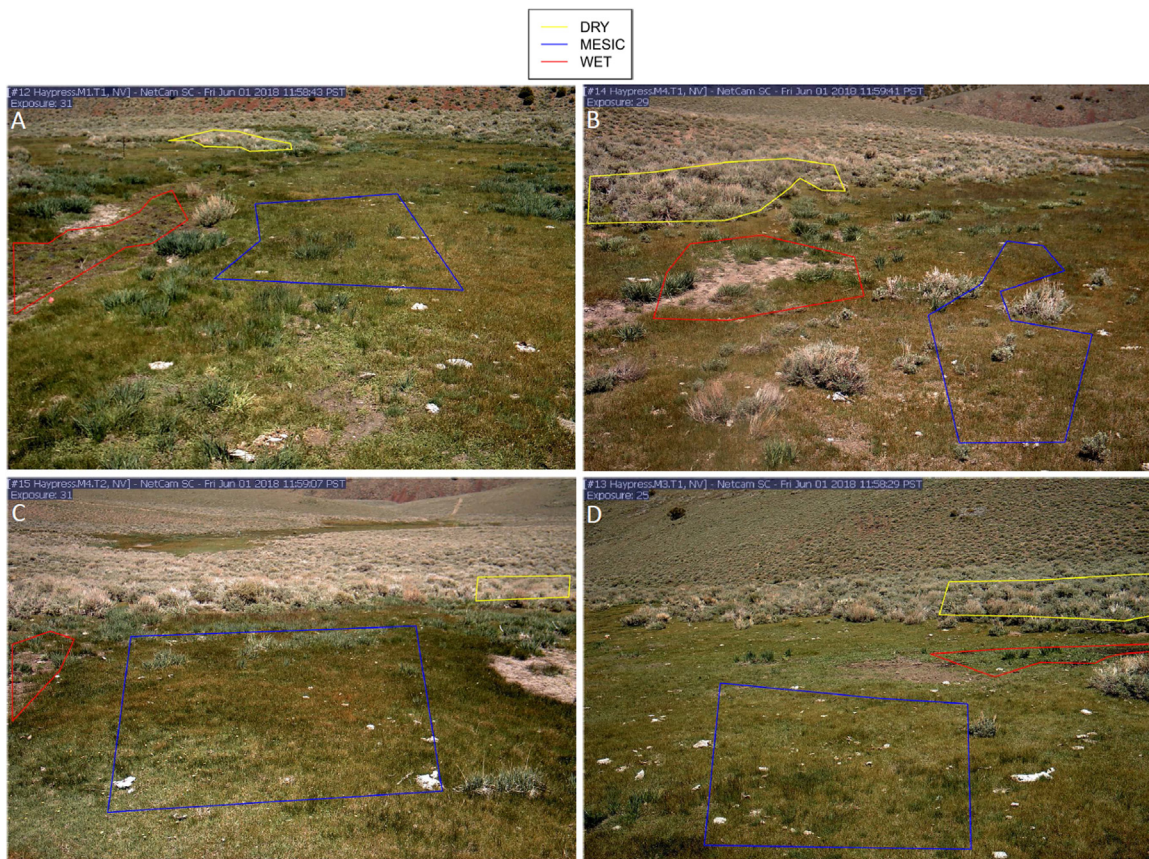


Figure 2. PhenoCam regions of interest (ROIs) for **A**, lower meadow, **B**, middle A meadow, **C**, middle B meadow, and **D**, upper meadow. Each ROI is outlined: dry meadows (shown in yellow), mesic meadow (shown in blue), and wet meadows (shown in red).

senescence line with the x-axis. Stabilization date and downturn date are fit based on predicted peak GCC from the slopes of the recovery and senescence line. Growing season length was determined by subtracting upturn date from the recession date.

Landsat NDVI and GPP

For comparisons of vegetation greenness and primary production estimated from satellite, we extracted Landsat NDVI and GPP at 30 m from different sources. NDVI from Landsat images was averaged over the meadow polygons (blue areas, see Fig. 1) for two time periods: years 2015 to 2018 for the Porter meadow and 2018 for the Haypress meadows with data from Landsat 8 using the Climate Engine (Huntington et al. 2017). The Porter and Haypress meadows occur at the intersection of adjacent Paths and Rows as part of the Worldwide Reference System for the Landsat sensor (Fig. S1, available online at [10.1016/j.rama.2022.12.001](https://doi.org/10.1016/j.rama.2022.12.001)). NDVI values were calculated as Equation 2:

$$NDVI = \frac{(NIR - Red)}{(NIR + Red)} \quad (2)$$

where *NIR* is the near infrared at-surface reflectance and *Red* is the red at-surface reflectance.

The full meadow polygons included dry, mesic, and wet meadow types within the camera viewsheds (see Fig. 1).

We used gross primary production (GPP) modeled data product by Robinson et al. (2018) available in Google Earth Engine (Gorelick et al. 2017) at 30-m spatial resolution for its ease of use. The GPP data product by Robinson et al. (2018) is based on the MOD17 algorithm (MODERate Resolution Imaging Spectroradiometer) (Running et al. 2004) applied to the Landsat time series and

more finely resolved inputs than the 500-m MODIS GPP data product. Landsat GPP is a 16-d cumulative product of GPP (kg-C-m^{-2}). We report GPP values as the mean of nine meadow pixels (30×30 m) centered on the PhenoCam locations for the four meadows in this study.

To capture the variation in seasonal amplitude (i.e., height of the growing season response curve) and variable growing season length, we integrated under the fitted seasonal GCC curve and the Landsat-derived GPP time series for the growing season dates between the upturn and recession dates defined by the phenopix-package. Integrated GCC (iGCC) and integrated GPP (iGPP) were determined by integrating the area under the respective curves between upturn and recession dates using the integrate function in the base R statistical package (R Core Team 2013). Annually integrated values for satellite iGPP and PhenoCam iGCC were compared to determine the relationship between satellite and PhenoCam metrics of productivity.

Statistical methods

We used a one-way analysis of variance (ANOVA) with meadow as the dependent variable and percent foliar cover by plant functional group as the independent variable to determine if there were functional group differences in vegetation cover across meadows. Three plant functional groups were present: shrubs, forbs, and graminoids. We also evaluated total percent foliar cover. We used a 1-way ANOVA to determine if within a meadow site there were differences in the percent foliar cover of functional groups. Plant height was analyzed using a repeated measures ANOVA with Tukey tests. Root mean square error (RMSE) and Pearson's *r* were used to determine the strength of the relation-

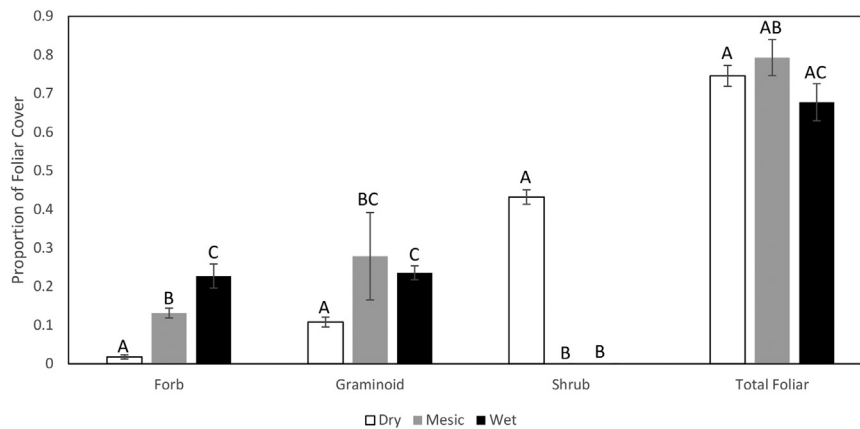


Figure 3. Line point intercept data grouped by percent foliar cover of functional type at the four meadows in the Haypress Meadow complex in the Desatoya Mountains, Nevada. Significant differences are indicated by uppercase letters among dry, mesic, and wet meadows.

Table 2

One-way analysis of variance for the difference in percent foliar cover of functional types across the three meadow types.

Forbs	Df	Sum Sq.	Mean Sq.	F value	Prob (> F)
Plot	2	0.5438	0.272	21.57	< 0.0001
Residuals	71	0.8951	0.013		
Graminoid					
Plot	2	0.332	0.166	5.116	0.0084
Residuals	71	2.304	0.032		
Shrub					
Plot	2	2.8127	1.406	237.8	< 0.0001
Residuals	71	0.4198	0.006		
Total foliar					
Plot	2	0.1831	0.092	4.79	0.0112
Residuals	71	1.3568	0.019		

ship between Landsat-derived NDVI and PhenoCam-derived GCC and the relationship between Landsat-derived GPP and PhenoCam GCC. All Landsat NDVI and GPP values were used to fit the RMSE and r values between PhenoCam GCC for the dates of the Landsat overpass. A simple linear regression was used to assess the relationship between iGCC and iGPP.

Results

Haypress meadows subregions

One-way ANOVAs determined that the four meadows in Haypress did not differ significantly by meadow location in terms of the percent foliar cover of the dominant functional groups. There was no difference in shrub, forb, graminoid, or total vegetation percent foliar cover between the four meadows. However, percent cover of functional groups was significantly different between dry, mesic, and wet meadows (Fig. 3, Table 2).

Dominant species in the dry meadow type were mountain big sagebrush (*Artemisia tridentata* Nutt. ssp. *vaseyana* [Rydb.] Beetle), and Douglas' sedge (*Carex douglasii* Boott). Mountain sagebrush was 35–40% and Douglas' sedge was 23–29% of the total cover. Other species < 10% but > 4% of the cover found in the dry meadows were *Leymus triticoides* (Buckley) Pilg., *Poa secunda* J. Presl, and *Poa pratensis* L. Mesic meadows were dominated by Douglas' sedge with foliar cover of 30–65%. Secondary dominant species varied by meadow and were *Juncus arcticus* Willd., *Poa secunda* J. Presl, *Poa pratensis* L., and *Chenopodium fremontii* S. Watson. Wet meadows were more varied and dominant species included *Carex nebrascensis* Dewey, *Carex douglasii* Boott, *Iris missouriensis* Nutt., *Ranunculus cymbalaria* Pursh, and *Juncus arcticus* Willd.

Porter meadow vegetation was measured in 2017, and composition was similar to the Haypress meadows (for details see Snyder et al. 2019). The dry meadow was dominated by mountain big sagebrush, big sagebrush (*Artemisia tridentata* sp. *tridentata*), Douglas' sedge, *Iva axillaris*, *Leymus cinereus*, and *Bromus tectorum*. The mesic meadow was dominated by Douglas' sedge and *J. arcticus*. The wet meadow was dominated by *C. nebrascensis* and *J. arcticus*.

Seasonal fits of GCC and phenophase dates within the three meadow types were remarkably similar for upturn date, stabilization date, and downturn date, with the least similarity in the end-of-season recession date (Fig. 4). The greatest divergence in phenophase dates was observed for recession date. Middle B had the longest growing season (Table 3) for both the dry and mesic meadow types.

In general, the dry meadow type had a later start to the growing season than the mesic and wet meadow types and longer growing season length (days \pm 1 SD) and lower seasonal amplitude in GCC (155 ± 33 , 0.3 ± 0.01 , respectively). This result was expected given that the dry meadow was dominated by semideciduous shrub species, instead of forbs and graminoids (see Fig. 4). Mesic meadows had the shortest growing season length and intermediate amplitude (87 ± 12 , 0.07 ± 0.01). Wet meadows had intermediate growing season length and the greatest amplitude in GCC (123 ± 30 , 0.10 ± 0.02). The longer growing season length in the upper wet meadow was due to the presence of *Iris* (*Iris missouriensis*) in the region of interest. *Iris* is largely unpalatable to grazers and a species indicative of meadow degradation and overgrazing (Brown 1982).

Field-estimated vegetation height reflects species composition and vegetation physiognomy (Fig. 5). Height in the dry meadows increased a bit and then was relatively stable through time, as would be expected from semideciduous shrub communities. The lower meadow had significantly greater vegetation height than the other three meadows (Table S1, available online at 10.1016/j.rama.2022.12.001). In the mesic meadows, height was very low by the end of the season (< 8.5 cm) and Middle B had significantly greater vegetation height than the other three meadows. Height in the wet meadows was generally < 10 cm. The exception to this was the Middle A meadow, which had increased height relative to the other three meadows. The increased height in Middle A was due to the presence of *Iris* (*I. missouriensis*) in the region of interest.

Greenness metrics from satellite and PhenoCam at meadow level

Comparisons of Landsat NDVI, Landsat GPP, and PhenoCam GCC metrics were conducted at the whole meadow level using the

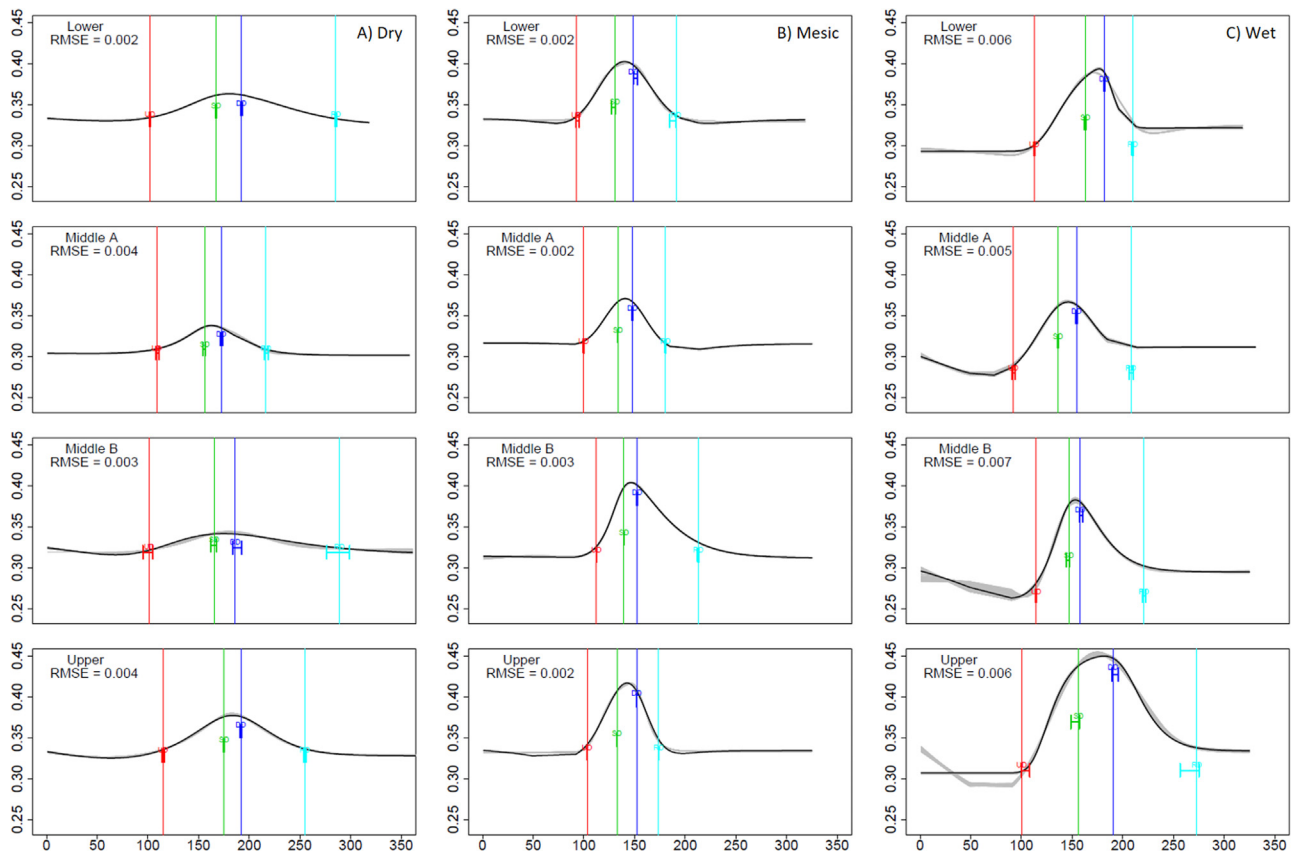


Figure 4. Green Chromatic Coordinate values and phenophase dates for the regions of interest for the three meadow types **A**, dry meadows, **B**, mesic meadows, and **C**, wet meadows. Phenophase dates and confidence intervals are upturn date (UD), a stabilization date (SD), a downturn date (DD), and a recession date (RD).

Table 3

Phenophase dates and confidence intervals for the three subregion meadow types. Phenophase dates and confidence intervals are upturn date (UD), stabilization date (SD), downturn date (DD), and recession date (RD). Growing season length (GSL) was determined by subtracting UD from RD. GSL and minimum, maximum, and amplitude values of Green Chromatic Coordinate (GCC).

Type & site	UD DOY ± (d)	SD	DD	RD	GSL D	Min GCC	Max	Amplitude
Dry—Lower	102 (0.69)	168 (0.43)	192 (0.83)	286 (0.78)	183	0.33	0.36	0.03
Dry—Middle A	108 (1.51)	156 (1.18)	174 (1.10)	219 (1.84)	107	0.31	0.34	0.03
Dry—Middle B	101 (4.71)	165 (2.70)	186 (4.52)	289 (11.12)	188	0.32	0.34	0.02
Dry—Upper	115 (1.08)	175 (0.45)	192 (0.90)	255 (0.95)	140	0.34	0.38	0.04
Mesic—Lower	93 (1.51)	131 (2.01)	153 (2.16)	191 (3.24)	98	0.34	0.40	0.07
Mesic—Middle A	100 (0.24)	134 (0.11)	148 (0.28)	181 (0.20)	81	0.32	0.37	0.05
Mesic—Middle B	112 (0.22)	140 (0.20)	153 (0.21)	213 (0.68)	100	0.33	0.40	0.08
Mesic—Upper	103 (0.23)	133 (0.28)	152 (0.13)	174 (0.16)	71	0.34	0.42	0.07
Wet—Lower	113 (0.41)	164 (0.85)	182 (0.22)	210 (0.64)	97	0.30	0.39	0.09
Wet—Middle A	94 (1.47)	137 (0.58)	155 (1.01)	211 (2.02)	116	0.29	0.37	0.08
Wet—Middle B	115 (0.51)	147 (1.71)	160 (1.30)	222 (1.41)	106	0.28	0.38	0.10
Wet—Upper	100 (4.21)	156 (4.30)	190 (2.84)	273 (9.30)	173	0.31	0.45	0.14

camera viewshed (see Fig. 1) and averaged across 30-m pixels; this approach evaluates metrics for each of four meadows across all three meadow types or subregions (dry, mesic, and wet). All the Haypress meadows were small and were 1 Landsat pixel, while the Porter meadow was 4 Landsat pixels. There was good agreement between Landsat NDVI and PhenoCam GCC for all four of the Haypress meadows in 2018 (Fig. 6 and Table 4, $r \geq 0.87$, and $RMSE \leq 0.05$). The Porter Canyon meadow spanned 4 years ranging from dry to wet rainfall years. Long-term average precipitation is 341 mm. Total annual precipitation in 2015 was below average (284 mm), and 2016 was above the long-term average (441 mm) following a 4-yr drought; 2017 precipitation exceeded long-term average (452 mm) and was followed in 2018 by a slightly below average yr (312 mm). NDVI values were highly

correlated with Landsat in the Porter Canyon meadow for 3 of the 4 years (Fig. 7 and Table 4, $r \geq 0.90$ and $RMSE \leq 0.05$). The exception to this was in 2016 with lower correlation and higher RMSE (see Fig. 7 and Table 4, $r=0.60$ and $RMSE=0.09$). In this year, Landsat NDVI greenness was sustained at a greater value in the fall, while GCC declined. This discrepancy may be due to the satellite essentially seeing something different than the PhenoCam. The satellite sees more ground area due to its nadir view, and the satellite has a greater spatial scale (90 × 90 m) than the field of view of the near surface PhenoCam. In 2015, there were far fewer Landsat images due to unusual and frequent small storms during the growing season. Consequently, one available image was excluded from the analyses (06/20/2015) because examination of the image determined it had relatively high cloud cover over

Table 4

Camera viewshed metrics are shown. Phenophase dates and confidence intervals for the meadows are upturn date (UD), stabilization date (SD), downturn date (DD), and recession date (RD). Growing season length (GSL) was determined by subtracting UD from RD. Minimum, maximum, and amplitude of seasonal GCC and integrated GCC (iGCC) are presented. Root mean square error (RMSE) and Pearson's correlation coefficient (*r*) between PhenoCam GCC and Landsat NDVI or Landsat GPP and the number of available Landsat images used in the analyses.

Meadow & Yr	UD	SD	DD	RD	GSL	Min	Max	Amp	iGCC	Pearson's <i>r</i> NDVI vs. GCC	RMSE NDVI vs. GCC	Pearson's <i>r</i> GPP vs. GCC	RMSE GPP vs. GCC	Prob NDVI vs. GCC	Prob > F GPP vs. GCC	N=# Landsat NDVI	N=# Landsat GPP
Lower 2018	100 (0.38)	134 (0.31)	152 (0.21)	196 (0.64)	97	0.33	0.4	0.07	35.79	0.95	0.03	0.89	68.3	< 0.001	< 0.0001	23	22
Middle A 2018	100 (0.22)	135 (0.12)	152 (0.59)	188 (0.27)	88	0.31	0.36	0.05	29.86	0.98	0.0045	0.87	68.62	< 0.001	< 0.0001	22	22
Middle B 2018	113 (0.27)	140 (0.21)	154 (0.26)	219 (0.73)	106	0.32	0.39	0.07	37.74	0.96	0.03	0.92	56.92	< 0.0001	< 0.0001	22	22
Upper 2018	102 (0.21)	135 (0.14)	148 (0.11)	202 (0.33)	99	0.33	0.4	0.07	36.78	0.87	0.05	0.93	56.39	< 0.0001	< 0.0001	22	22
Porter 2015	112 (1.19)	157 (0.77)	194 (3.08)	292 (6.84)	179	0.32	0.37	0.04	61.03	0.9	0.006	0.94	37.96	< 0.0084	< 0.0001	12	22
Porter 2016	84 (1.30)	147 (0.44)	160 (0.34)	265 (16.93)	181	0.33	0.37	0.04	63.62	0.61	0.09	0.97	34.96	< 0.001	< 0.0001	26	22
Porter 2017	103 (0.51)	155 (0.22)	225 (1.00)	298 (0.41)	190	0.33	0.37	0.04	68.66	0.91	0.01	0.97	36.11	< 0.0001	< 0.0001	24	22
Porter 2018	108 (0.78)	152 (0.32)	161 (0.54)	301 (2.50)	190	0.33	0.37	0.04	66.16	0.94	0.05	0.96	37.81	< 0.0001	< 0.0001	24	22

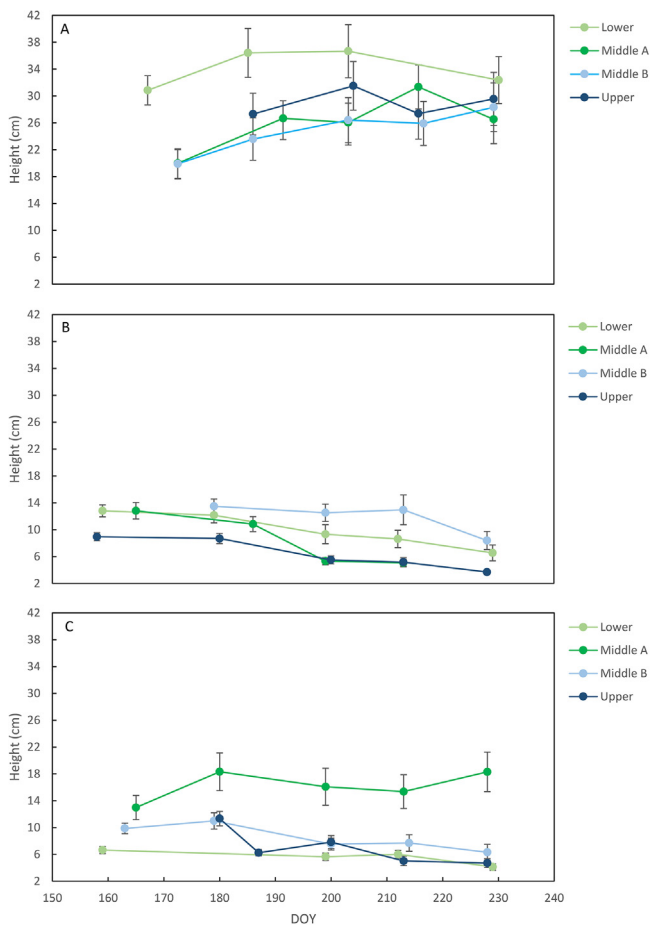


Figure 5. Mean plant height (± 1 standard deviation) measured throughout the 2018 growing season on fixed transects with day of year (DOY) in the x-axis in **A**, the dry meadows, **B**, mesic meadows, and **C**, wet meadows.

the Porter Canyon meadow. The data point is still shown in the figure for reference (see Fig. 7). There was greater variation in the phenophase dates across the different years than what was found for the Haypress meadows in a single year. In particular, although peak greenness was reached consistently by late May and early June, the length of time until downturn date varied. In 2015, the growing season was characterized by frequent small storms that appear to have increased the length of time of peak greenness. Likewise, the wet yr of 2017 also had increased length of peak greenness.

Landsat GPP was highly correlated with PhenoCam GCC. For all four Haypress meadows in 2018, Pearson's r ranged from 0.87 to 0.93 (see Table 4). In the Porter meadow, the Pearson's r ranged from 0.94 to 0.97 (see Table 4). The linear relationship between iGCC and iGPP was strong ($R^2 = 0.89$) across a gradient of grazing pressure (Fig. 8). Uncontrolled grazing practices at Haypress meadows were reflected in lower values for both iGCC and iGPP. Middle A, which was a preferred meadow by the cattle, had the lowest values, and Middle B, the least accessible to cattle, had the highest values for the Haypress meadows. In contrast, managed cattle grazing (or lack of grazing for 2 years) in Porter Canyon was reflected in greater values for both iGCC and iGPP. In 2016, an average precipitation yr, cattle were excluded from the meadow (S. Lossing, Smith Creek Ranch, personal communication) and iGCC and iGPP had the second highest values. Porter Canyon meadow had values that were nearly double that of Haypress, with the wet yr of 2017 having the highest values.

Discussion

We determined that it was possible to satisfy our first objective and use PhenoCams to quantify baseline phenological profiles for heavily grazed Great Basin meadow communities that spanned an aridity gradient ranging from wet to mesic to dry meadows (see Fig. 4). The greatest divergence in phenophase dates for each sub-region was for the recession dates. Plausible explanations for these differences include differing levels of grazing pressure and/or water availability. Middle B had the longest growing season for both the dry and mesic meadow types (see Table 3), and although we made no formal estimates of grazing pressure, during the 2018 growing season, cattle were routinely present in the Middle A meadow. The Middle B meadow is located up a steeper slope (≈ 15 -degree slope). It is the smallest meadow and appears to have the least use by cattle. In general, PhenoCam GCC curves for the Haypress meadows had the least amplitude and longest growing season length in the dry communities; greater amplitude in GCC and the shortest growing season length in the mesic communities; and the greatest amplitude and greatest variability in growing season length in the wet communities.

In terms of evaluating our second objective, to establish baseline measures of plant cover and height, we found meadow elevation or location did not have a significant effect on the percentage of cover of the dominant functional groups, but there was a significant effect of meadow type on the percent foliar cover of the dominant functional groups. Mesic and wet meadows had greater cover of graminoids than dry meadows. Wet meadows had the greatest percent foliar cover of forbs. Height was highest in the dry shrub-dominated communities, moderate and variable in the wet communities, and lowest in the mesic communities.

The near surface PhenoCams reflected differences in greenness and productivity between sites with different grazing histories and were highly correlated with satellite values for NDVI and modeled GPP. PhenoCam greenness (GCC) complemented Landsat-based depictions of productivity (GPP) and vegetation vigor (NDVI) (Browning et al. 2021). These strong relationships support our third objective, to quantify the relationships between the different platforms. Furthermore, while they provide similar information, these two platforms would be considered complementary—as PhenoCams increase temporal resolution, Landsat increases spatial resolution (Browning et al. 2021).

Next, we explore objective 4, whether remotely sensed phenology metrics from PhenoCam and Landsat can distinguish differences in grazing pressure. In the following sections, we explore the interpretations of 1) grazing pressure and data from the three meadow and subregions at Haypress and 2) observations of grazing pressure at the scale of the full meadows using both sensor platforms and Haypress and Porter Meadows.

Observations along an aridity gradient for Haypress Meadows

The PhenoCams were not designed to monitor grazing pressure, but images were inspected visually for the presence of grazers; only horse and cattle were observed in the daily images. Between May 1 and August 31, 2018, either horses or cattle were observed in images 12, 17, 3, and 10 d in the Lower, Middle A, Middle B, and Upper meadows, respectively. This crude estimate of grazing pressure cannot fully explain differences in meadow growing season phenology but does indicate that Middle B meadow had less grazing pressure, which seems reasonable given that it is the smallest of the four meadows and grazers must climb a fairly steep slope through sagebrush to reach the meadow.

Snyder et al. (2016) analyzed GCC of the subregions of meadow types (dry, mesic, and wet) for the growing season of 2015 in the Porter meadow. Results for the three meadow types' GCC values

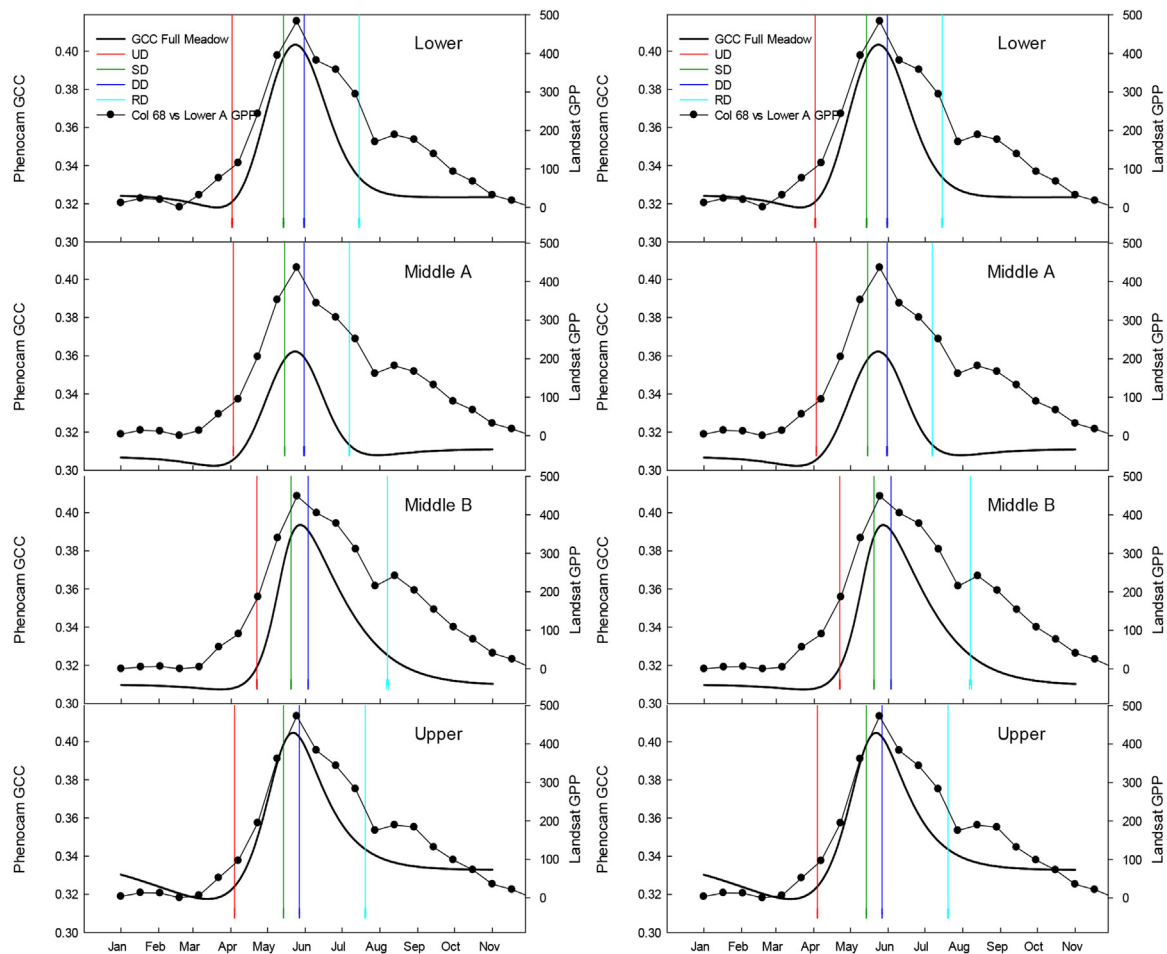


Figure 6. Data for the Haypress camera viewshed regions of interest (ROI). The relationship between Landsat-derived normalized vegetation difference index (NDVI) plotted as all available dates (black dots) and PhenoCam-fitted Green Chromatic Coordinate (GCC) (black line) and phenophase dates derived from PhenoCam imagery (vertical lines), as well as the relationship between Landsat-derived gross primary production (GPP) (black dots) and PhenoCam-fitted GCC (black line). Phenophase dates and confidence intervals are upturn date (UD), a stabilization date (SD), a downturn date (DD), and a recession date (RD). Landsat data before April were removed due to snow.

ranged from 0.327 to 0.389, similar to what was demonstrated in Haypress. Growing season length was 130, 157, and 181 d in the wet, mesic, and dry meadows, respectively, which is similar to what was found for growing season length in Haypress for wet and dry meadows (123 and 155 d, respectively); but the growing season length for mesic meadows in Haypress was only on average 87 d, illustrating the potential disproportionate effect of chronic feral horse grazing in mesic meadows. Other studies have demonstrated variation in growth response to grazing as a function of plant community type. Clary (1995) observed that sedge-dominated sites (similar to the mesic communities seen in this study) had lower height growth and biomass following defoliation than other sites grazed similarly. These differences in response could be due to different grazing tolerances of species, water availability, variability in litter reduction across sites, or lack of defoliation during the “boot” stage (i.e., the time when the seedhead is enclosed within the sheath of the flag leaf) of species (Miller et al. 1990; Moore et al. 1991; Skaer et al. 2013; Richardson et al. 2021).

Observations at the Full Meadow Scale

PhenoCams proved useful for monitoring community phenology in heavily grazed meadow systems. The unfenced Haypress meadows have a 12-mo grazing season by free-roaming feral horses. In addition, there is cattle grazing on a 2-yr rotation. For 2 years,

these meadows are grazed by cattle from mid-April through June. The next 2 yr they are grazed by cattle from July through September. In 2018, approximately 700 calf-cow pairs had access to Haypress meadows from July through September. Porter meadow is fenced, and the canyon is gated. There is no grazing by feral horses, and grazing by cattle is managed. Smith Creek Ranch records indicated that in 2015 and 2016, the meadow gate remained closed and there was no grazing by cattle. In 2017, cows entered and grazed the Porter meadow from July 5 to July 10, when all 32 cows were removed. Between July 27 and August 21, additional cows entered the meadow and 27 cows were removed. The gate was closed. In 2018, the gate to the meadow was opened on July 31. Sixty cows were removed on August 1, 12 cows were removed August 29, and 7 cows were removed on September 19. Then the gate was closed.

Differences between the timing and duration of grazing by different types of grazers were detected in both the PhenoCam GCC and Landsat-derived GPP, validating our hypothesis that these remote sensing tools can be useful in monitoring the outcomes of grazing management. Increased grazing pressure reduced integrated GCC and GPP (see Fig. 8). Furthermore, there was a strong linear relationship between iGCC and iGPP, even though these two platforms operate at vastly different spatial and temporal scales (daily and 16-d). Chronic grazing of the Haypress meadows reduced iGCC and iGPP by approximately 50% relative to a managed

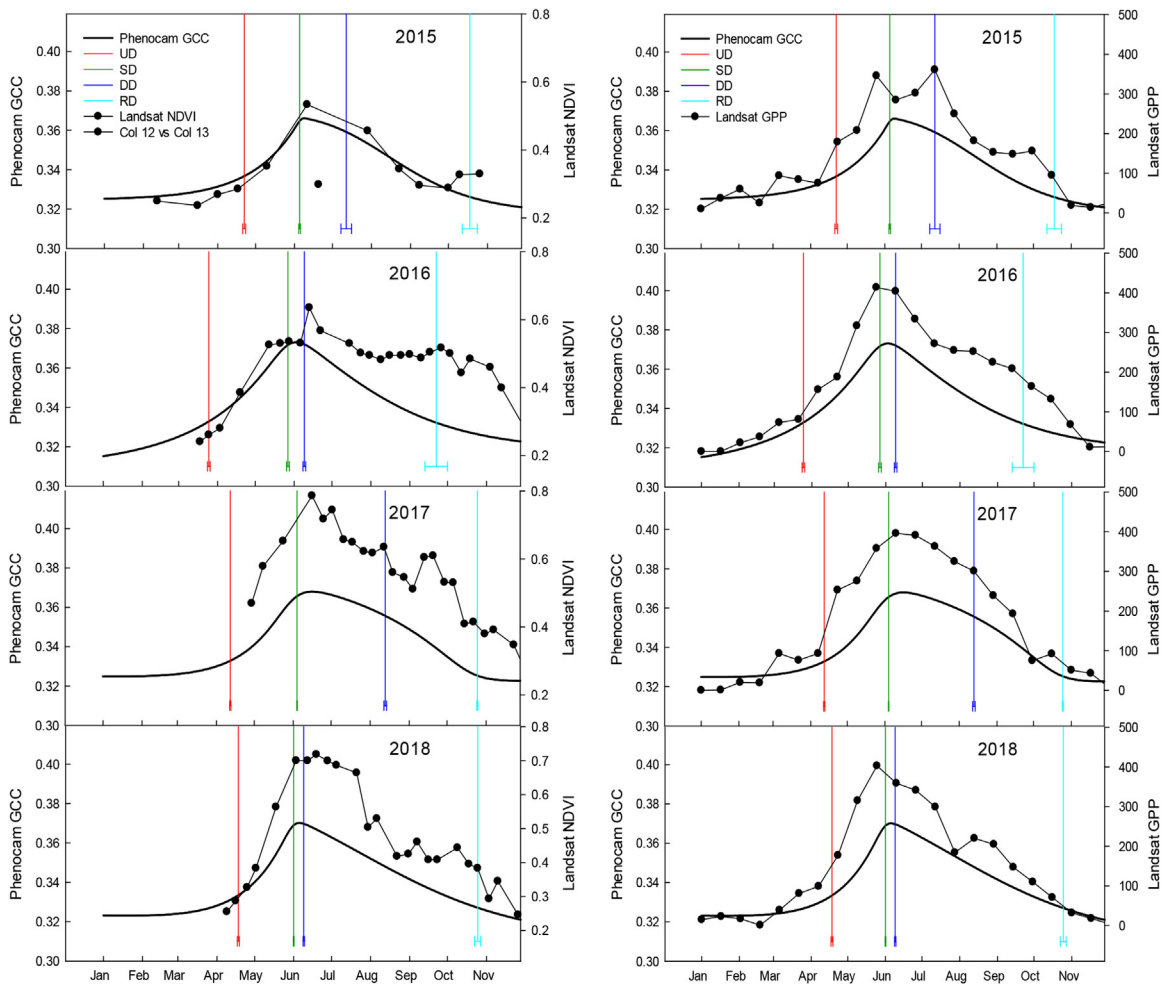


Figure 7. Data for the Porter meadow camera viewed regions of interest (ROI). The relationship between Landsat-derived normalized vegetation difference index (NDVI) plotted as all available dates NDVI (black dots) and PhenoCam-fitted Green Chromatic Coordinate (GCC) (black line) and phenophase dates derived from PhenoCam imagery (vertical lines), as well as the relationship between Landsat-derived GPP (black dots) and PhenoCam-fitted GCC (black line). Phenophase dates and confidence intervals are upturn date (UD), a stabilization date (SD), a downturn date (DD), and a recession date (RD). Landsat data before April were removed due to snow.

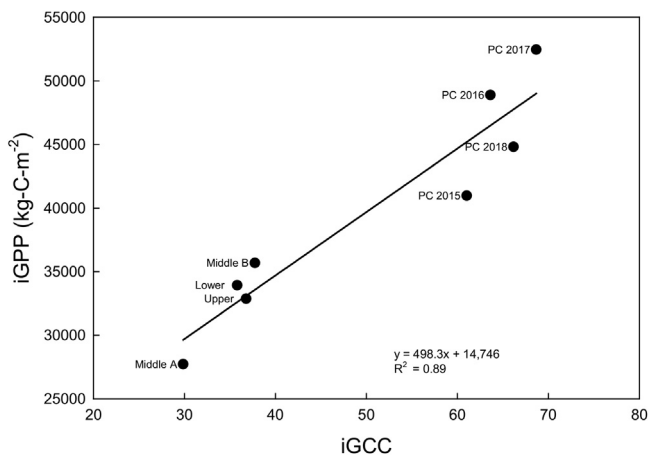


Figure 8. Relationship between integrated PhenoCam Green Chromatic Coordinate (iGCC) and Landsat gross primary production (iGPP) for the camera viewed regions of interest.

grazing situation. Consistently, studies have demonstrated negative relationships between chronic or overgrazing and plant growth metrics. In a literature review conducted by Vernon et al. (2022), they found that out of 15 studies looking at grazing plant inter-

actions in high-elevation meadows, 12 had some negative correlation between chronic grazing and plant growth/community metrics. Interpretations of patterns in satellite-based GPP (Robinson et al. 2018) are supported by high correlations between the Robinson et al. (2018) GPP data product with GPP estimated via eddy-covariance methods across grasslands and shrublands (Pearson's $r = 0.66$ and 0.74 , respectively). The ability to detect differences in grazing intensity using 30-m data products is notable and likely influenced by high productivity meadow systems. Future research will evaluate these relationships in more arid grazed rangeland systems.

Chronic horse grazing with the addition of cattle in late summer appeared to produce a distinct end to the growing season, as evidenced by the more symmetrical GCC curves in Haypress relative to the more asymmetrical curves in the Porter meadow that have a skewed distribution with an elongated tail in the fall season (Figures 6 and 7). In addition, there was more variance in the 90th percentile of the phenophase dates in the Porter meadow. It seems reasonable that uniformly grazed graminoids and forbs < 10 cm in height would turn brown more abruptly, whereas nonuniform ungrazed or lightly grazed vegetation would have a more gradual transition to senescence. Defoliation of graminoids has been found in some cases to hasten senescence (Becker et al. 1997). Han et al. (2015) showed that grazing shifted senescence timing of several observed species and shrank the overall growing period for the

communities in their study. It has been well studied that grazing can have positive, zero, or negative effects on plant communities depending on a variety of factors such as grazing intensity, water availability, season of grazing, and available soil nutrients (Noy-Meir 1993).

The Porter meadow, located lower in elevation than the Haypress meadows, had a much longer growing season in 2018; the growing season length was nearly twice as long (see Table 4). While this may be partially attributable to weather difference due to elevation, it could also be due to differences in grazing season and duration, types of grazers, soil water availability, and/or differences in soil nutrients (Aerts and Berendse 1988; Berdanier and Klein 2011). Visual inspection of the images from Haypress show little evidence of cattle grazing early in the season and an absence of fresh manure piles. However, as previously mentioned, horse grazing occurs year-round. There are indications of grazing by cattle from July through the end of August with increased frequency of fresh manure in the camera viewsheds, and as mentioned previously, horse grazing is year-round. Because of the short growing season length of the mesic meadows (they were largely senesced by the time cattle reached the meadows), it seems reasonable to postulate that the mesic meadows may be more impacted by feral horse grazing than cattle. Future research will address the role of grazing versus soil water availability on meadow growing season length.

Visual inspection of the PhenoCam images show clearly reduced plant height in the Haypress meadows relative to the Porter meadow (see Fig. S1). Vegetation height measurements at Haypress showed low height of vegetation (Fig. 5). Yet we were still able to use PhenoCams to track seasonal phenology. There were strong correlations between PhenoCam GCC and Landsat NDVI and GPP; this shows promise for developing statistical models to extrapolate to other Great Basin meadows systems using the Landsat archive. Landsat NDVI was well correlated with PhenoCam GCC. However, in 2018, there was a gap in May and June likely due to cloudy images, and consequently Landsat NDVI did not capture the peak of the growing season. There was also a gap in Landsat NDVI in 2015 and 2017 in the Porter meadow that missed the peak of season. The 16-d overpass and obstruction by clouds are two prominent shortcomings of Landsat, albeit less so in this case where the study area occurs at the intersection of multiple Landsat scenes (Fig. S2, available online at [10.1016/j.rama.2022.12.001](https://doi.org/10.1016/j.rama.2022.12.001)). The greater temporal resolution of the PhenoCams improved the utility of this platform for capturing the peak of the growing season. The ability to detect overgrazing from chronic overgrazing is promising for the Great Basin, which has a large-scale feral horse problem (Boyd et al. 2017; Beever et al. 2018). Our results are in concurrence with other studies that found feral horses preferred groundwater-dependent ecosystems and that feral horse grazing can reduce height and cover of vegetation (Ganskopp and Vavra 1986; Crane et al. 1997; Beever and Brussard 2000).

Implications

Groundwater-dependent ecosystems provide an array of ecosystem goods and services, although they are a small fraction of the total landscape in semiarid and arid landscapes. In the current study we found that GDEs can be successfully monitored with PhenoCams at small spatial and temporal scales and by Landsat platform metrics for NDVI and GPP. Effects of chronic overgrazing were detected by metrics from both platforms, and integrated GCC and GPP values were particularly adept at summarizing seasonal patterns of phenology into a concise measure of ecosystem function. These findings are consistent with previous work on these meadow systems that looked at the utility of PhenoCams and Landsat to assess the ecological condition of meadows (Snyder et al. 2016;

Carroll et al. 2017; Browning et al. 2019; Snyder et al. 2019b). PhenoCam metrics were useful at both the subregion meadow type level and the level of the full meadow. PhenoCam metrics at the full meadow scale were in good agreement with NDVI and GPP derived from Landsat at the 30 × 30 m scale. Our results are in agreement with other research on GDEs in the semiarid western United States, which found that Landsat NDVI was able to track the success of restoration projects in GDEs. Successful restoration of GDEs found restoration efforts increased NDVI relative to pre-restoration NDVI, presumably due to increased water availability that improved plant vigor (Huntington et al. 2016; Fesenmyer et al. 2018; Hausner et al. 2018; Wilson and Norman 2018). The establishment of these baseline conditions from PhenoCams and Landsat images, in conjunction with field-based measures of plant composition and height, will allow us to track community responses of these meadows to management that excludes feral horse grazing and uses precision management of livestock.

Declaration of Competing Interest

The authors declare that they have no known competing financial interests or personal relationships that could have appeared to influence the work reported in this paper.

Acknowledgments

Guillermo Ponce-Campos assisted with MODIS GPP data extraction. MODIS GPP products (Robinson et al. 2018) are available as Google Earth Engine ImageCollection IDs UMT/NTSG/v2/MODIS/GPP. We thank Smith Creek Ranch, Bureau of Land Management, and The Nature Conservancy for access to federal and private land and the conservation easement.

Supplementary materials

Supplementary material associated with this article can be found, in the online version, at doi:[10.1016/j.rama.2022.12.001](https://doi.org/10.1016/j.rama.2022.12.001).

References

- Aerts, R., Berendse, R., 1988. The effect of increased nutrient availability on vegetation dynamics in wet heathlands. *Vegetatio* 76, 63–69.
- Badgley, G., Field, C.B., Berry, J.A., 2017. Canopy near-infrared reflectance and terrestrial photosynthesis. *Science Advances* 3, e1602244.
- Badik, K.J., Saito, L., Byer, S., Provencher, L., 2019. Ecological departure of TNC-mapped groundwater dependent ecosystems. Report by The Nature Conservancy.
- Bailey, D., 2004. Management strategies for optimal grazing distribution and use of arid rangelands. *Journal of Animal Science* 82, E147–E153.
- Becker, G.F., Busso, C.A., Montani, T., Orchansky, A., Brevedan, R.E., Burgos, M., Flemmer, A.C., 1997. Effects of defoliating *Stipa tenuis* and *Piptochaetium napostaense* at different phenological stages: tiller demography and growth. *Journal of Arid Environments* 35, 251–268.
- Beever, E.A., Brussard, P.F., 2000. Examining ecological consequences of feral horse grazing using exclosures. *Western North American Naturalist* 60, 236–254.
- Beever, E.A., Huntsinger, L., Petersen, S.L., 2018. Conservation challenges emerging from free-roaming horse management: a vexing social-ecological mismatch. *Biological Conservation* 226, 321–328.
- Berdanier, A.B., Klein, J.A., 2011. Growing season length and soil moisture interactively constrain high elevation aboveground net primary production. *Ecosystems* 14, 963–974.
- Bestelmeyer, B.T., Duniway, M.C., James, D.K., Burkett, L.M., Havstad, K.M., 2013. A test of critical thresholds and their indicators in a desertification-prone ecosystem: more resilience than we thought. *Ecology Letters* 16, 339–345.
- Boyd, C., Davies, K., Collins, G., 2017. Impacts of feral horse use on herbaceous riparian vegetation within a sagebrush steppe ecosystem. *Rangeland Ecology & Management* 70, 411–417.
- Bradley, B.A., Mustard, J.F., 2008. Comparison of phenology trends by land cover class: a case study in the Great Basin, USA. *Global Change Biology* 14, 334–346.
- Briske, D.D., Richards, J.H., 1995. Plant responses to defoliation: a physiological, morphological and demographic evaluation. In: Bedunah, D., Sosebee, R. (Eds.), *Wildland plants: physiological ecology developmental morphology*. Society for Range Management, Denver, CO, USA, pp. 635–710.

- Brown, D.E., 1982. Montane meadow grassland. In: Brown, D.E. (Ed.), *Desert plants. Biotic communities of the American southwest United States and Mexico*. University of Arizona, Tucson, AZ, USA, pp. 113–114.
- Brown, J., Bach, L., Aldous, A., Wyers, A., DeGagné, J., 2011. Groundwater-dependent ecosystems in Oregon: an assessment of their distribution and associated threats. *Frontiers in Ecology the Environment* 9, 97–102.
- Brown, L.A., Dash, J., Ogutu, B.O., Richardson, A.D., 2017. On the relationship between continuous measures of canopy greenness derived using near-surface remote sensing and satellite-derived vegetation products. *Agricultural and Forest Meteorology* 247, 280–292.
- Brown, T.B., Hultine, K.R., Steltzer, H., Denny, E.G., Denslow, M.W., Granados, J., Henderson, S., Moore, D., Nagai, S., SanClements, M., Sánchez-Azofeifa, A., Sonnen-tag, O., Tazik, D., Richardson, A., 2016. Using PhenoCams to monitor our changing Earth: toward a global PhenoCam network. *Frontiers in Ecology and the Environment* 14, 84–93.
- Browning, D.M., Karl, J.W., Morin, D., Richardson, A.D., Tweedie, C.E., 2017. PhenoCams bridge the gap between field and satellite observations in an arid grassland ecosystem. *Remote Sensing* 9, 1071.
- Browning, D.M., Rango, A., Karl, J.W., Laney, C.M., Vivoni, E.R., Tweedie, C.E., 2015. Emerging technological and cultural shifts advancing drylands research and management. *Frontiers in Ecology and the Environment* 13, 52–60.
- Browning, D.M., Russell, E.S., Ponce-Campos, G.E., Kaplan, N., Richardson, A.D., Seyednasrollah, B., Spiegel, S., Saliendra, N., Alfieri, J.G., Baker, J., 2021. Monitoring agroecosystem productivity and phenology at a national scale: a metric assessment framework. *Ecological Indicators* 131, 108147.
- Browning, D.M., Snyder, K.A., Herrick, J.E., 2019. Plant phenology: taking the pulse of rangelands. *Rangelands* 41, 129–134.
- Burke, M.W., Rundquist, B.C., 2021. Scaling PhenoCam GCC, NDVI, and EVI2 with harmonized Landsat-Sentinel using Gaussian processes. *Agricultural and Forest Meteorology* 300, 108316.
- Caldwell, M., 1984. Plant requirements for prudent grazing. Developing strategies for rangeland management. National Research Council/National Academy of Sciences. Westview Press, Boulder, CO, USA, pp. 117–152.
- Carroll, R.W., Huntington, J.L., Snyder, K.A., Niswonger, R.G., Morton, C., Stringham, T.K., 2017. Evaluating mountain meadow groundwater response to pinyon-juniper and temperature in a Great Basin watershed. *Ecology* 10, e1792.
- Clary, W.P., 1995. Vegetation and soil response to grazing simulation on riparian meadows. *Rangeland Ecology & Management* 48, 18–25.
- Cleland, E.E., Chuine, I., Menzel, A., Mooney, H.A., Schwartz, M.D., 2007. Shifting plant phenology in response to global change. *Trends in Ecology and Evolution* 22, 357–365.
- Crane, K.K., Smith, M.A., Reynolds, D., 1997. Habitat selection patterns of feral horses in southcentral Wyoming. *Journal of Range Management* 374–380.
- Cremonese, E., Filippa, G., Galvagno, M., Siniscalco, C., Oddi, L., di Cella, U.M., Migliavacca, M., 2017. Heat wave hinders green wave: the impact of climate extreme on the phenology of a mountain grassland. *Agricultural and Forest Meteorology* 247, 320–330.
- Cui, T., Martz, L., Lamb, E.G., Zhao, L., Guo, X., 2019. Comparison of grassland phenology derived from MODIS satellite and PhenoCam Near-Surface Remote Sensing in North America. *Canadian Journal of Remote Sensing* 45, 707–722.
- Devitt, D., Bird, B., Lyles, B., Fenstermaker, L., Jasoni, R., Strachan, S., Biondi, F., Mensing, S., Saito, L., 2018. Assessing near surface hydrologic processes and plant response over a 1600 m mountain valley gradient in the Great Basin, NV, USA. *Water* 10, 420.
- Devitt, D., Fenstermaker, L., Young, M.H., Conrad, B., Baghzouz, M., Bird, B., 2011. Evapotranspiration of mixed shrub communities in phreatophytic zones of the Great Basin region of Nevada (USA). *Ecology* 4, 807–822.
- Eamus, D., Zolfaghari, S., Villalobos-Vega, R., Cleverly, J., Huete, A., 2015. Groundwater-dependent ecosystems: recent insights from satellite and field-based studies. *Hydrology Earth System Sciences*.
- Elmore, A.J., Manning, S.J., Mustard, J.F., Craine, J.M., 2006. Decline in alkali meadow vegetation cover in California: the effects of groundwater extraction and drought. *Journal of Applied Ecology* 43, 770–779.
- Fesenmyer, K.A., Dauwalter, D.C., Evans, C., Allai, T., 2018. Livestock management, beaver, and climate influences on riparian vegetation in a semi-arid landscape. *PLoS One* 13, e0208928.
- Filippa, G., Cremonese, E., Migliavacca, M., Galvagno, M., Forkel, M., Wingate, L., Tomelleri, E., Di Cella, U.M., Richardson, A.D., 2016. Phenopix: AR package for image-based vegetation phenology. *Agricultural Forest Meteorology* 220, 141–150.
- Ganskopp, D., Vavra, M., 1986. Habitat use by feral horses in the Northern sagebrush steppe. *Rangeland Ecology & Management* 39, 207–212.
- General Accounting Office, 1988. Public rangelands: some riparian areas restored but widespread improvements will be slow. US Accounting Office, Resources, Community and Economic Development Division, Washington, DC, USA, p. 85 B-230548.
- General Accounting Office, 1988. Public rangelands: some riparian areas restored but widespread improvements will be slow. Report GAO/RCED-88-105. Washington, DC, USA: US General Accounting Office, Resources, Community and Economic Development Division. 85 p.
- Garrott, R.A., 2018. Wild horse demography: implications for sustainable management within economic constraints. *Human–Wildlife Interactions* 12. doi:10.26077/z7w0-0w34.
- Gorelick, N., Hancher, M., Dixon, M., Ilyushchenko, S., Thau, D., Moore, R., 2017. Google Earth Engine: Planetary-scale geospatial analysis for everyone. *Remote Sensing of Environment* 202, 18–27.
- Gu, L., Post, W.M., Baldocchi, D.D., Black, T.A., Suyker, A.E., Verma, S.B., Vesala, T., Wofsy, S.C., 2009. Characterizing the seasonal dynamics of plant community photosynthesis across a range of vegetation types. *Phenology of ecosystem processes*. Springer, New York, NY, USA, pp. 35–58.
- Han, J., Chen, J., Xia, J., Li, L., 2015. Grazing and watering alter plant phenological processes in a desert steppe community. *Plant Ecology* 216, 599–613.
- Hall, F.D., Bryant, L., 1995. Herbaceous stubble height as a warning of impending cattle grazing damage to riparian areas. US Department of Agriculture, Forest Service, Pacific Northwest Research Station, Portland, OR, USA, p. 9 Gen. Tech. Rep. PNW-GTR-362.
- Harrill, J.R., Welch, A.H., Prudic, D.E., Thomas, J.M., Carman, R.L., Plume, R.W., Gates, J.S., Mason, J.L., 1983. Aquifer systems in the Great Basin region of Nevada, Utah, and adjacent states: a study plan. US Geological Survey, Washington, DC, USA.
- Hausner, M.B., Huntington, J.L., Nash, C., Morton, C., McEvoy, D.J., Pilliod, D.S., Hegewisch, K.C., Daudert, B., Abatzoglou, J.T., Grant, G., 2018. Assessing the effectiveness of riparian restoration projects using Landsat and precipitation data from the cloud-computing application ClimateEngine. *Ecological Engineering* 120, 432–440.
- Herrick, J.E., Van Zee, J.W., Havstad, K.M., Burkett, L.M., Whitford, W.G., 2005. Monitoring manual for grassland, shrubland and savanna ecosystems. Volume I: quick start. Volume II: design, supplementary methods and interpretation. USDA-ARS Jornada Experimental Range. USDA-ARS Jornada Experimental Range, Las Cruces, New Mexico, USA.
- Huang, S., Tang, L., Hupy, J.P., Wang, Y., Shao, G., 2021. A commentary review on the use of normalized difference vegetation index (NDVI) in the era of popular remote sensing. *Journal of Forestry Research* 32, 1–6.
- Hufkens, K., Keenan, T.F., Flanagan, L.B., Scott, R.L., Bernacchi, C.J., Joo, E., Brunzell, N.A., Verfaillie, J., Richardson, A.D., 2016. Productivity of North American grasslands is increased under future climate scenarios despite rising aridity. *Nature Climate Change* 6, 710–714.
- Huntington, J., Hegewisch, K.C., Daudert, B., Morton, C., Abatzoglou, J., McEvoy, D.J., Erickson, T., 2017. Climate engine: cloud computing of climate and remote sensing data for enhanced natural resource monitoring and process understanding. *Bulletin of the American Meteorological Society* 98, 2397–2410.
- Huntington, J., McGwire, K., Morton, C., Snyder, K., Peterson, S., Erickson, T., Niswonger, R., Carroll, R., Smith, G., Allen, R., 2016. Assessing the role of climate and resource management on groundwater dependent ecosystem changes in arid environments with the Landsat archive. *Remote Sensing of Environment* 185, 186–197.
- Julitta, T., Cremonese, E., Migliavacca, M., Colombo, R., Galvagno, M., Siniscalco, C., Rossini, M., Fava, F., Cogliati, S., di Cella, U.M., 2014. Using digital camera images to analyse snowmelt and phenology of a subalpine grassland. *Agricultural and Forest Meteorology* 198, 116–125.
- Kauffman, J.B., Krueger, W.C., 1984. Livestock impacts on riparian ecosystems and streamside management implications ... a review. *Journal of Range Management* 37, 430–438.
- Khishigbayar, J., Fernández-Giménez, M.E., Angerer, J.P., Reid, R.S., Chantsalkham, J., Baasandorj, Y., Zumberelmaa, D., 2015. Mongolian rangelands at a tipping point? Biomass and cover are stable but composition shifts and richness declines after 20 years of grazing and increasing temperatures. *Journal of Arid Environments* 115, 100–112.
- Klos, P.Z., Link, T.E., Abatzoglou, J.T., 2014. Extent of the rain-snow transition zone in the western US under historic and projected climate. *Geophysical Research Letters* 41, 4560–4568.
- Lebon, A., Mailleret, L., Dumont, Y., Grogard, F., 2014. Direct and apparent compensation in plant-herbivore interactions. *Ecological Modelling* 290, 192–203.
- Lowry, C.S., Loheide II, S.P., Moore, C.E., Lundquist, J.D., 2011. Groundwater controls on vegetation composition and patterning in mountain meadows. *Water Resources Research* 47.
- Miller, R.F., Haferkamp, M.R., Angell, R.F., 1990. Clipping date effects on soil water and regrowth in crested wheatgrass. *Rangeland Ecology & Management* 43, 253–257.
- Moore, K., Moser, L.E., Vogel, K.P., Waller, S.S., Johnson, B., Pedersen, J.F., 1991. Describing and quantifying growth stages of perennial forage grasses. *Agronomy Journal* 83, 1073–1077.
- Naiman, R.J., Decamps, H., Pollock, M., 1993. The role of riparian corridors in maintaining regional biodiversity. *Ecological Applications* 3, 209–212.
- Naumburg, E., Mata-Gonzalez, R., Hunter, R.G., McLendon, T., Martin, D.W., 2005. Phreatophytic vegetation and groundwater fluctuations: a review of current research and application of ecosystem response modeling with an emphasis on Great Basin vegetation. *Environmental Management* 35, 726–740.
- Noy-Meir, I., 1993. Compensating growth of grazed plants and its relevance to the use of rangelands. *Ecological Applications* 3, 32–34.
- Pérez Hoyos, I.C., Krakauer, N.Y., Khanbilvardi, R., Armstrong, R.A., 2016. A review of advances in the identification and characterization of groundwater dependent ecosystems using geospatial technologies. *Geosciences* 6, 17.
- Phillips, L.B., Hansen, A.J., Flather, C.H., 2008. Evaluating the species energy relationship with the newest measures of ecosystem energy: NDVI versus MODIS primary production. *Remote Sensing of Environment* 112, 4381–4392.
- PRISM Climate Group, 2021. PRISM Climate Data Available at.
- R Core Team, 2013. R: a language and environment for statistical computing (version 3.5.3) R Foundation for Statistical Computing Available at.
- Reynolds, J.F., Smith, D.M.S., Lambin, E.F., Turner, B.L., Mortimore, M., Batterbury, S.P., Downing, T.E., Dowlatabadi, H., Fernández, R.J., Herrick, J.E., Huber-Sannwald, E., Jiang, H., Leemans, R., Lynam, T., Maestre, F.T., Aiyar, M., Walker, B., 2007.

- Global desertification: building a science for dryland development. *Science* 316 (5826), 847–851.
- <https://phenocam.nau.edu/webcam/>. PhenoCam: An ecosystem phenology camera network. Accessed on 05 May 2013.
- Richardson, A.D., Braswell, B.H., Hollinger, D.Y., Jenkins, J.P., Ollinger, S.V., 2009. Near-surface remote sensing of spatial and temporal variation in canopy phenology. *Ecological Applications* 19, 1417–1428.
- Richardson, W., Stringham, T.K., Lieurance, W., Snyder, K.A., 2021. Changes in meadow phenology in response to grazing management at multiple scales of measurement. *Remote Sensing* 13, 4028.
- Robinson, N.P., Allred, B.W., Smith, W.K., Jones, M.O., Moreno, A., Erickson, T.A., Nangle, D.E., Running, S.W., 2018. Terrestrial primary production for the conterminous United States derived from Landsat 30 m and MODIS 250 m. *Remote Sensing in Ecology Conservation* 4, 264–280.
- Rohde, M.M., Freund, R., Howard, J., 2017. A global synthesis of managing groundwater dependent ecosystems under sustainable groundwater policy. *Groundwater* 55, 293–301.
- Running, S.W., Nemani, R.R., Heinsch, F.A., Zhao, M., Reeves, M., Hashimoto, H., 2004. A continuous satellite-derived measure of global terrestrial primary production. *Bioscience* 54, 547–560.
- Sada, D., 2008. Great Basin riparian and aquatic ecosystems. In: Chambers, J.C., Devoe, N., Evenden, A. (Eds.), Collaborative management research in the great basin—examining the issues developing a framework for action. US Department of Agriculture, Forest Service, Rocky Mountain Research Station, Fort Collins, CO, USA, pp. 49–52.
- Scanlon, B.R., Levitt, D., Reedy, R.C., Keese, K., Sully, M., 2005. Ecological controls on water-cycle response to climate variability in deserts. *Proceedings of the National Academy of Sciences* 102, 6033–6038.
- Scanlon, B.R., Stonestrom, D.A., Reedy, R.C., Leaney, F.W., Gates, J., Cresswell, R.G., 2009. Inventories and mobilization of unsaturated zone sulfate, fluoride, and chloride related to land use change in semiarid regions, southwestern United States and Australia. *Water Resources Research* 45.
- Sinai, N.L., Coates, P.S., Andrie, K.M., Jefferis, C., Senties-Cué, C.G., Pitesky, M.E., 2017. A serosurvey of greater sage-grouse (*Centrocercus urophasianus*) in Nevada, USA. *Journal of Wildlife Diseases* 53, 136–139.
- Skaer, M.J., Graydon, D.J., Cushman, J.H., 2013. Community-level consequences of cattle grazing for an invaded grassland: variable responses of native and exotic vegetation. *Journal of Vegetation Science* 24, 332–343.
- Snyder, K., Wehan, B., Filippa, G., Huntington, J., Stringham, T., Snyder, D., 2016. Extracting plant phenology metrics in a great basin watershed: methods and considerations for quantifying phenophases in a cold desert. *Sensors* 16, 1948.
- Snyder, K.A., Evers, L., Chambers, J.C., Dunham, J., Bradford, J.B., Loik, M.E., 2019a. Effects of changing climate on the hydrological cycle in cold desert ecosystems of the Great Basin and Columbia Plateau. *Rangeland Ecology & Management* 72, 1–12.
- Snyder, K.A., Huntington, J.L., Wehan, B.L., Morton, C.G., Stringham, T.K., 2019b. Comparison of Landsat and land-based phenology camera Normalized Difference Vegetation Index (NDVI) for dominant plant communities in the Great Basin. *Sensors* 19, 1139.
- Sonnentag, O., Hufkens, K., Teshera-Sterne, C., Young, A.M., Friedl, M., Braswell, B.H., Milliman, T., O’Keefe, J., Richardson, A.D., 2012. Digital repeat photography for phenological research in forest ecosystems. *Agricultural and Forest Meteorology* 152, 159–177.
- Stringham, T.K., Krueger, W.C., Thomas, D.R., 2001. Application of non-equilibrium ecology to rangeland riparian zones. *Journal of Range Management* 210–217.
- Tang, J., Körner, C., Muraoka, H., Piao, S., Shen, M., Thackeray, S.J., Yang, X., 2016. Emerging opportunities and challenges in phenology: a review. *Ecosphere* 7.
- Toda, M., Richardson, A.D., 2018. Estimation of plant area index and phenological transition dates from digital repeat photography and radiometric approaches in a hardwood forest in the Northeastern United States. *Agricultural and Forest Meteorology* 249, 457–466.
- Torregrosa, A., Devoe, N., 2008. Urbanization and changing land use in the Great Basin. In: Chambers, J.C., Devoe, N., Evenden, A. (Eds.), Collaborative management research in the Great Basin—examining the issues developing a framework for action. US Department of Agriculture, Forest Service, Rocky Mountain Research Station, Fort Collins, CO, USA, pp. 9–13.
- Tucker, C.J., Elgin Jr., J., McMurtrey III, J., Fan, C., 1979. Monitoring corn and soybean crop development with hand-held radiometer spectral data. *Remote Sensing of Environment* 8, 237–248.
- Vernon, M.E., Campos, B.R., Burnett, R.D., 2022. Effects of livestock grazing on the ecology of Sierra meadows: a review of the current state of scientific knowledge to inform meadow restoration and management. *Environmental Management* 69, 1118–1136.
- Vrieling, A., Meroni, M., Darvishzadeh, R., Skidmore, A.K., Wang, T., Zurita-Milla, R., Oosterbeek, K., O’Connor, B., Paganini, M., 2018. Vegetation phenology from Sentinel-2 and field cameras for a Dutch barrier island. *Remote Sensing of Environment* 215, 517–529.
- Wilson, N.R., Norman, L.M., 2018. Analysis of vegetation recovery surrounding a restored wetland using the normalized difference infrared index (NDII) and normalized difference vegetation index (NDVI). *International Journal of Remote Sensing* 39, 3243–3274.
- Zhao, D., Xu, M., Liu, G., Ma, L., Zhang, S., Xiao, T., Peng, G., 2017. Effect of vegetation type on microstructure of soil aggregates on the Loess Plateau, China. *Agriculture, Ecosystems & Environment* 242, 1–8.